Journal of Alloys and Compounds 501 (2010) 275–281

Contents lists available at ScienceDirect

Journal of Alloys and Compounds

journal homepage: www.elsevier.com/locate/jallcom

Synthesis and characterization of hollow MoS_2 microspheres grown from MoO_3 precursors

Guowei Li, Changsheng Li*, Hua Tang, Kesheng Cao, Juan Chen, Fangfei Wang, Yue Jin

College of Material Science and Engineering, Jiangsu University, Zhenjiang 212013, PR China

ARTICLE INFO

Article history:
Received 7 December 2009
Received in revised form 13 April 2010
Accepted 15 April 2010
Available online 22 April 2010

Keywords:
MoO_3 macrobelts
MoS_2 microspheres
Hydrothermal

ABSTRACT

Mono-dispersed molybdenum disulfide (MoS_2) microspheres with the diameter of 2–4 μm have been successfully synthesized with MoO_3 as precursors by a hydrothermal method. The precursors, long and smooth MoO_3 macrobelts, were synthesized through a facile route. The combined techniques of X-ray diffraction (XRD), energy dispersive (EDS), scanning electron microscope (SEM), transmission electron microscope (TEM), Raman spectra, and UV–visible spectrophotometer (UV–vis) were used for characterization of the as-prepared MoS_2. It was found that the MoS_2 microspheres were assembled by MoO_3 macrobelts and the belts-like structure of the precursor played a crucial role on the formation of the MoS_2 microstructures in our experiment. A possible formation mechanism of the hollow sphere-like MoS_2 structure was preliminarily presented on the basis of the experimental facts.

1. Introduction

One-dimensional solid nanostructural materials, such as nanorods, nanotubes and nanobelts, have been the focus of extensive studies worldwide because of their potential application in nanodevices [1] and functional materials [2]. Compared with these nanostructures, the hollow-sphere materials are expected to be applied in a broad range of areas, such as delivery vehicles for the controlled release of various substances. These include drugs, cosmetics, dyes, and inks, and for the protection of fillers, catalysts, and pigments due to their advantageous properties like low density, large specific area, mechanical and thermal stability, and surface permeability [3–6]. Therefore, a variety of chemical and physicochemical approaches have been employed to prepare hollow spheres, such as: self-assembly routes [7], sonochemical process [8], hydrothermal method [9], emulsion/interfacial polymerization strategies [10], and template-assisting techniques including "hard templates," such as silica spheres [11], polystyrene microspheres [12], and "soft templates," such as vesicles [13], and emulsion droplets [14].

Transition metal sulfide molybdenum disulfide (MoS_2), for its unique layered structures consisting of covalently bound S–Mo–S trilayers, continues to attract the most interest for its important applications in solid lubricants [15], potential hydrogen storage [16], solid-state secondary lithium battery cathodes [17], and field emission tips [18]. To date, various methods were put forward to prepare MoS_2 including thermal decomposition [19], hydrothermal or solvothermal synthesis [20,21], electronbeam irradiation activation [22], sonochemical process [23], and template synthesis [24] with different molybdenum sources such as: Na_2MoO_4, $(NH_4)_6Mo_7O_{24}{\cdot}4H_2O$, $(NH_4)_2MoS_4$ MoO_3 [25,26,27,28]. Among the above approaches, many types of MoS_2 micro/nano materials with various morphologies, such as inorganic fullerene-like and nanotubes, nanorods, nanowires, nanosheets, nanoflowers were obtained. However, few research studies on the fabrication of MoS_2 hollow spheres were done, and the existing methods are fascinating. However, to some extent, they also possess some disadvantages, such as: the use of toxic reagent, poor dispersity and nonuniform size in product. Therefore, it is highly desirable to develop a simple synthesis method, which can control the diameter of the product and require mild conditions, ease of operation and a benign environmentally.

In this paper, we report a novel and simple low temperature hydrothermal method for the preparation of MoS_2 microspheres using MoO_3 macrobelts as precursors. Analysis of the result materials shows that the produced MoS_2 microspheres are hollowed with diameters of 2–4 μm. Tetrabutyl ammonium bromide's templating mechanism is presented for the formation of MoS_2 hollow microspheres under the hydrothermal process.

2. Experimental details

2.1. Synthesis of MoO_3 macrobelts

All reagents were analytical grade. The preparation procedure was as follows: 20 mmol of $Na_2MoO_4{\cdot}2H_2O$ was dissolved in 10 mL distilled water. Then 16 mL perchloric acid (4 mol/L) was added slowly into the sodium molybdate solution at a speed of 20–25 s/drop under violent stirring. After that, the resulting solution was

* Corresponding author.
E-mail addresses: leegowek@163.com (G. Li), lichangsheng@ujs.edu.cn (C. Li).

0925-8388/$ – see front matter © 2010 Elsevier B.V. All rights reserved.
doi:10.1016/j.jallcom.2010.04.088

transferred into a 50 mL Teflon-lined stainless autoclave. Hydrothermal reaction was carried out at 140 °C for 24 h. The lightblue precipitates were collected, washed with distilled water, and finally dried in vacuum at 80 °C for 8 h.

2.2. Synthesis of hollow MoS_2 microspheres

In a typical synthesis, 0.432 g of the as-prepared molybdenum trioxide (MoO_3) macrobelts was put into 30 mL of distilled water under continuous stirring. After 10 min, 0.252 g sodium fluoride (NaF), 0.290 g tetrabutyl ammonium bromide ($C_{16}H_{36}BrN$) and 0.972 g potassium thiocyanate (NaSCN) were added to the above solution and adjusted for a pH value to 6 with 2 mol/L HCl, the mixture was then transferred into a 50 mL Teflon-lined stainless steel autoclave. The autoclave was maintained at 200 °C for 12 h and naturally cooled down to room temperature. The solid products were filtered, rinsed with distilled water and absolute ethanol several times. Finally the products were dried in vacuum at 80 °C for 12 h.

2.3. Electrochemical measurements

X-ray diffraction (XRD) was recorded by using a D8 advance (Bruker-AXS) diffractometer, with Cu Kα radiation (λ = 1.5406 Å) at a scanning rate of 0.02/s; Scanning electron microscope (SEM) images were obtained by a JEOL JSM-7001F field emission scanning electron microscope (FESEM); Transmission electron microscopy (TEM) studies were carried out using a Japanese JEM-100CX II transmission electron microscopy. Roman spectra were taken under ambient conditions using a Roman spectrometer (In via, λ_{exc} = 532 nm). A glass substrate was used as the sample holder. UV–vis absorption was recorded on a SHIMADZU UV-2450 UV–visible spectrophotometer.

3. Results and discussions

3.1. Sample characterization

The XRD pattern of MoO_3 macrobelts is shown in Fig. 1. All the peaks can be indexed to orthorhombic-phase MoO_3 (JCPDS No. 35-0609, a = 0.3963 nm, b = 1.3856 nm, c = 0.3697 nm, space group *Pbnm*). The strong diffraction peaks of (0 2 0), (0 4 0), and (0 6 0) planes reveal a layered crystal structure or a highly anisotropic growth of the oxides. Scanning electron microscopy (SEM) indicates that the obtained MoO_3 consists of many smooth macrobelts

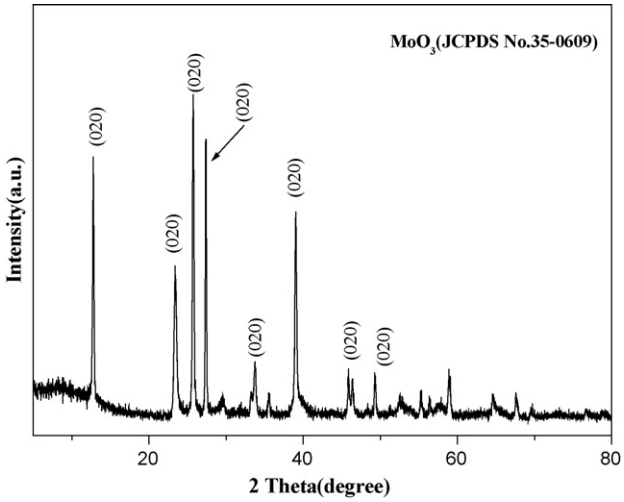

Fig. 1. XRD pattern of the obtained MoO_3 macrobelts.

with average width of about 0.5 μm (Fig. 2a and b). The width-to-thickness ratios were about 2–16, and the length of the products are up to 8 μm estimated from the TEM image (Fig. 2c), which was consistent with the SEM images. Deduced from the preferred orientation of (0 1 0) plane revealed by XRD and the belt-like morphology shown by SEM, it is suggested that macrobelts are grown along the (0 0 1) direction. Such crystallographic feature of MoO_3 microbelts are the same as α-MoO_3 nanocrystals reported by Xia et al. [29].

Fig. 3 shows the XRD patterns of the as-prepared MoS_2 microspheres via hydrothermal synthesis at 200 °C (Fig. 3a), calcined at 700 °C for 1 h (Fig. 3b), and 750 °C for 1 h (Fig. 3c) under Ar flow. It can be seen that the sample directly obtained from the autoclave (a) was of amorphous structure and only a relatively weak characteristic peak (0 0 2) was found, which indicated the poor-stacked

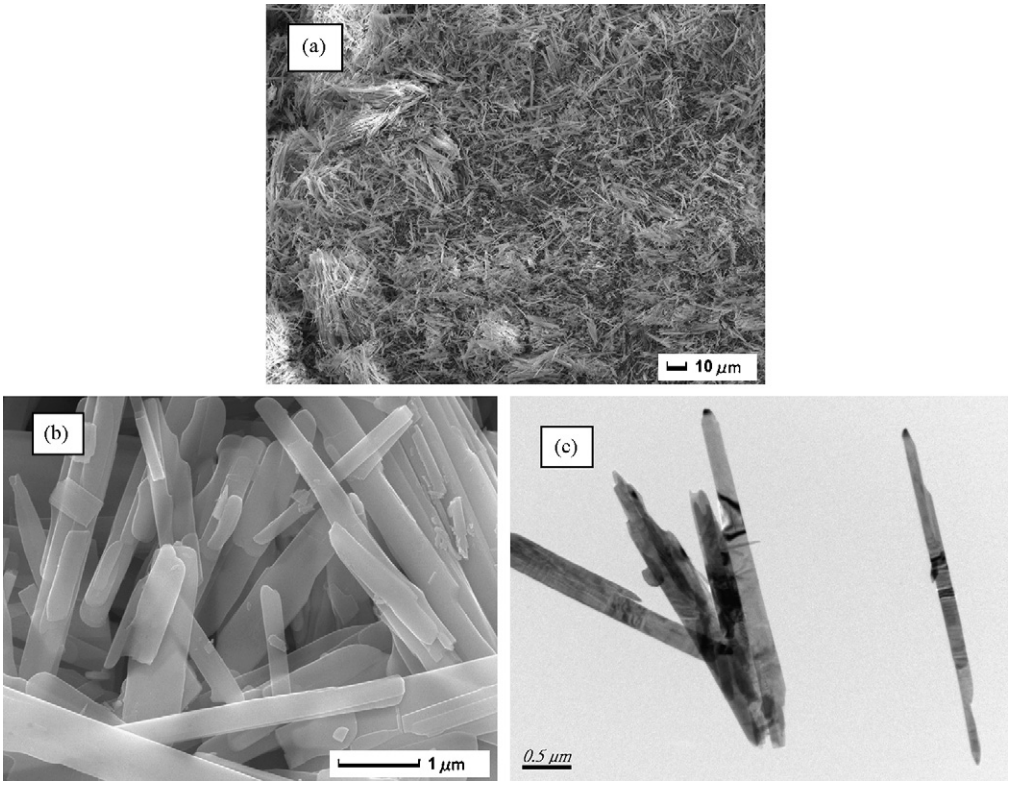

Fig. 2. (a and b) Typical SEM images of the MoO_3 macrobelts. (c) The TEM image of the products.

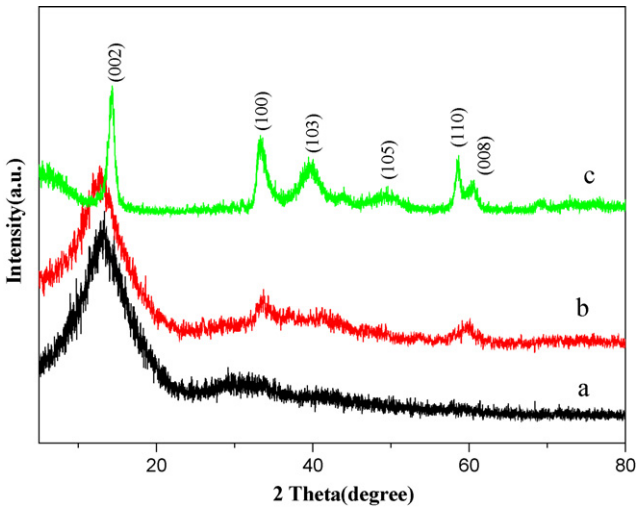

Fig. 3. XRD patterns of (a) as-synthesized MoS_2 microspheres without being annealed; (b) the samples annealed at 700 °C for 1 h; (c) the samples annealed at 750 °C for 1 h.

layered structure of MoS_2. This can be explained by the randomness and the tensile force of the crystals. It has been reported that the crystallinity of the MoS_2 prepared by hydrothermal route could be improved by annealing at high temperature [30]. Fig. 3b shows that the XRD pattern of the as-prepared MoS_2 annealed at 700 °C for 1 h under the flow of Ar, the existence of (0 0 2), (1 0 0) and (1 1 0) peaks indicating the formed of IF-MoS_2, but all the peaks are very weak. With the annealing temperature increasing to 750 °C (Fig. 3c), the peak of (0 0 2) became high and sharp, which indicates that the well-stacked layered structure of MoS_2 formed during the annealing process. And all of the diffraction peaks can be readily indexed to the hexagonal phase of MoS_2 (JCPDS No. 37-1492) with lattice constants $a = 3.161$ Å, $b = 3.161$ Å, $c = 12.84$ Å. The shift of the (0 0 2) peak in the XRD pattern, which is usually regarded as a key mechanism for strain relief of the folded structure, was observed in our investigation [31]. In our experiment, the (0 0 2) peak shifted to lower angle from 13.5° to 13.2° after annealed at 700 °C compared to that (14.38°) of hexagonal 2H-MoS_2. The value is much larger than that previously reported before (ca. 2%) [28], which may indicate strain with higher degree deriving from the curvature of the layers.

The morphologies of the MoS_2 products were primarily investigated by SEM measurement. Fig. 4a and b show that the obtained samples were microspheres dominating with an average diameter of about 4 μm (few of them are 1–2 μm), along with several broken hollow spheres. A High-magnification SEM image (Fig. 4c) shows a typical hollow sphere, indicating that the spheres are hollowed, and the thickness of the hollow-sphere shell is about 150 nm. It should be noted that the shell consists of several layers and can be regarded as a nestification of several hollow spheres. Some scientists vividly called them "onion" structure [32] or "Russian doll" structures. This is very crucial to understanding the formation mechanism. The EDS of SEM images of MoS_2 powder was shown in Fig. 4d, which was the direct evidence for the conclusion that except for Mo and S (elements of MoS_2), no other elements such as O, (elements of MoO_2) existed. Moreover, according to quantitative analysis of EDS, the molar ratio of Mo to S was found 1:2.07, which was almost consistent with the stoichiometric MoS_2 within experimental error.

The structural characterization and the hierarchical nature of the MoS_2 microspheres were further examined by TEM and high-resolution TEM (HRTEM) observations. Fig. 5a shows several spheres, which furthermore prove the hollow structure of the as-prepared MoS_2. What should be noted is that the structures in our experiment have many defects, this can be seen from the varying distances between the planes and bent lattice planes (as shown in Fig. 5b), to our knowledge, the existence of these defects may help to release some strain in the folded layer. More details for MoS_2

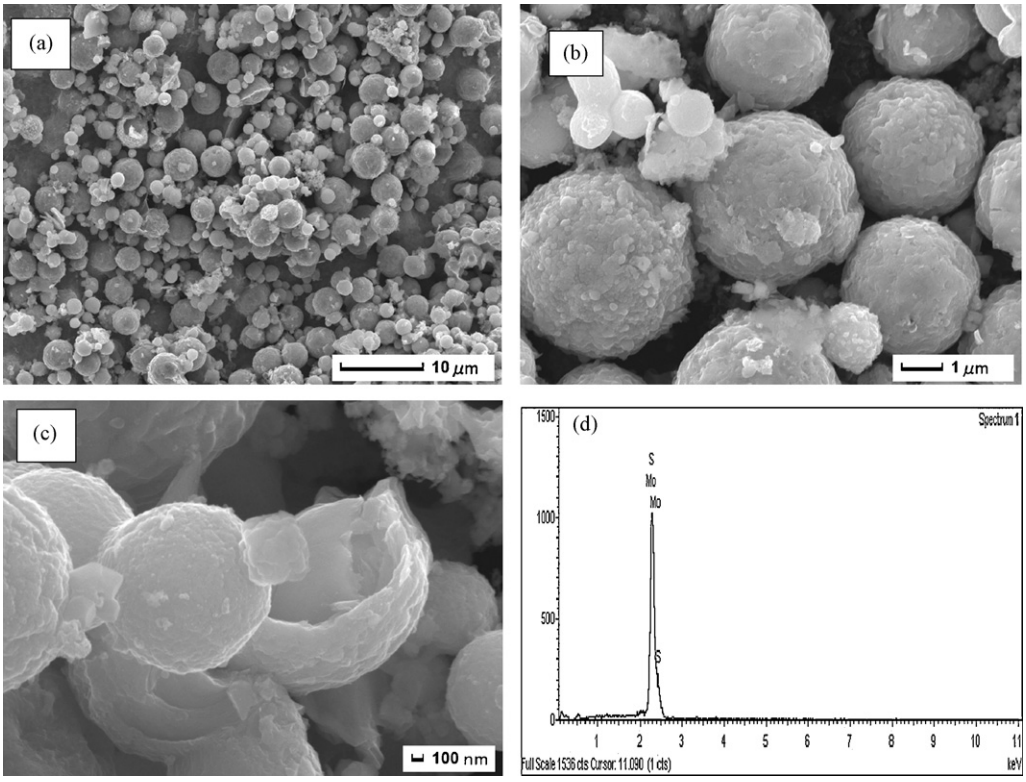

Fig. 4. SEM, EDS spectra of the MoS_2 macrostructures obtained via a hydrothermal route.

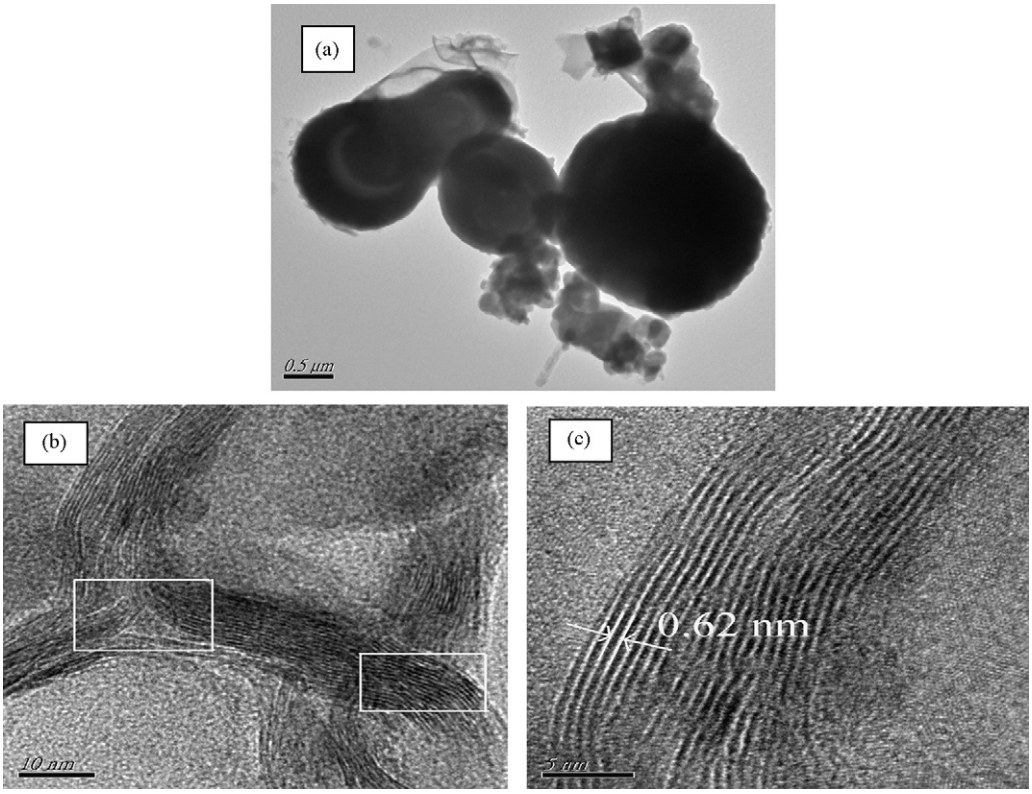

Fig. 5. TEM (a) and HRTEM (b) and (c) images of the MoS_2 annealed at 700 °C for 1 h under the flow of Ar.

after annealed are illustrated by HRTEM studies in Fig. 5c, which indicate the IF structure of the products with several layers. As a mean value of the distance between the two lattice fringes, the (0 0 2) planes, is 0.62 nm.

Further studies revealed that the initial concentration of $C_{16}H_{36}BrN$ had great influence on the evolution of MoS_2 morphologies. For example, when no $C_{16}H_{36}BrN$ was added and kept other reaction conditions constant, only belt-like products were obtained (Fig. 6a). Magnified SEM image (Fig. 6b) further reveals that the dimensions of the products were in accordance with that of the MoO_3 precursors. This can be explained by the facts that without the presence of $C_{16}H_{36}BrN$, no vessels were formed in the reaction process, so the morphology of the MoO_3 macrobelts did not change significantly. Increasing $C_{16}H_{36}BrN$ concentration to 0.01 M, spherical structures with the diameter of about 4 μm were formed (Fig. 6c), but the proportion of this structure is rather low. Fig. 6d is a representative SEM image of the product as-prepared at a higher $C_{16}H_{36}BrN$ concentration, namely 0.15 M, from the image, the diameter of the hollow nanospheres is estimated to be 4 μm also. However, once the concentration of $C_{16}H_{36}BrN$ was increased to 0.3 M, the aggregation of MoS_2 particles is seriously and the dispersion property is bad (as shown in Fig. 6e and f). Too low concentration (such as 0.01 M) and too high concentration (such as 0.3 M) of $C_{16}H_{36}BrN$ all could not lead to the formation of hollow spheres with good dispersion. The latter may be due to that the intercalating and intertwisting among these high molecules cannot be neglected, which lead to a high surface free energy of the MoS_2 particles, thus make the aggregation rather serious. The influence of the solvent was also investigated in our experiment. Fig. 7 showed the SEM images of the products prepared with pure ethanol as solvent. It can be seen that nearly all of them were of a spherical morphology, but with good dispersion and smaller particle size (2 μm). A Magnified SEM image (Fig. 7b) indicated that the surface of the MoS_2 sphere is rather rough. The possible reasons maybe lies in the fact that in the pure ethanol system, it is easy to achieve super-saturation, which is beneficial to the formation of small nanoparticles. Furthermore, in the nucleation and growth process, the existence of the ethanol solvent can prevent the hard aggregation between the non-bridging hydroxyl group and the particle surface. However, our present understanding of the formation mechanism to the MoS_2 sphere in the system of pure ethanol is still limited, more in-depth studies are in progress.

Fig. 8 displays the typical Raman spectra of the unannealed and annealed MoS_2 samples. It can be seen that the unannealed MoS_2 sample has two main peaks at about 378 cm^{-1} and 404 cm^{-1}, whereas, the annealed MoS_2 sample has three main peaks at about 286 cm^{-1}, 380 cm^{-1} and 406 cm^{-1}. According to Verble's research [33], Raman peaks of hexagonal phase of MoS_2 appeared at about 287 cm^{-1}, 383 cm^{-1} and 409 cm^{-1}. It is thus certain that the Raman peaks in Fig. 6 are attributable to hexagonal MoS_2. The Raman peak intensities of the annealed MoS_2 sample are stronger than those of the unannealed indicated the high crystallinity of the annealed MoS_2 sample, which are all in accordance with the XRD report. The UV–vis spectrum of the bulk MoS_2 and as-prepared MoS_2 spheres is shown in Fig. 9. It displays stronger absorption in the blue region and weaker absorption in the red region. Compared with the bulk MoS_2 (340 nm), the absorption peaks for the hollow spheres are markedly blue-shift (335). These suggest that the hollow macrospheres have obvious quantum confinement effect, which is also consistent with the results of XRD.

3.2. Formation mechanism

Based on the experimental procedures and the results, we believed that it was an $C_{16}H_{36}BrN$'s templating mechanism that should be responsible for the formation of MoS_2 as illustrated in Fig. 10. On the research of the growth process of the hollow structures using ionic liquids, Nakashima and Kimizuka [34] concluded that the ionic liquids (ILs) could form many micro-sized droplets in the solution under proper experimental conditions. In our experi-

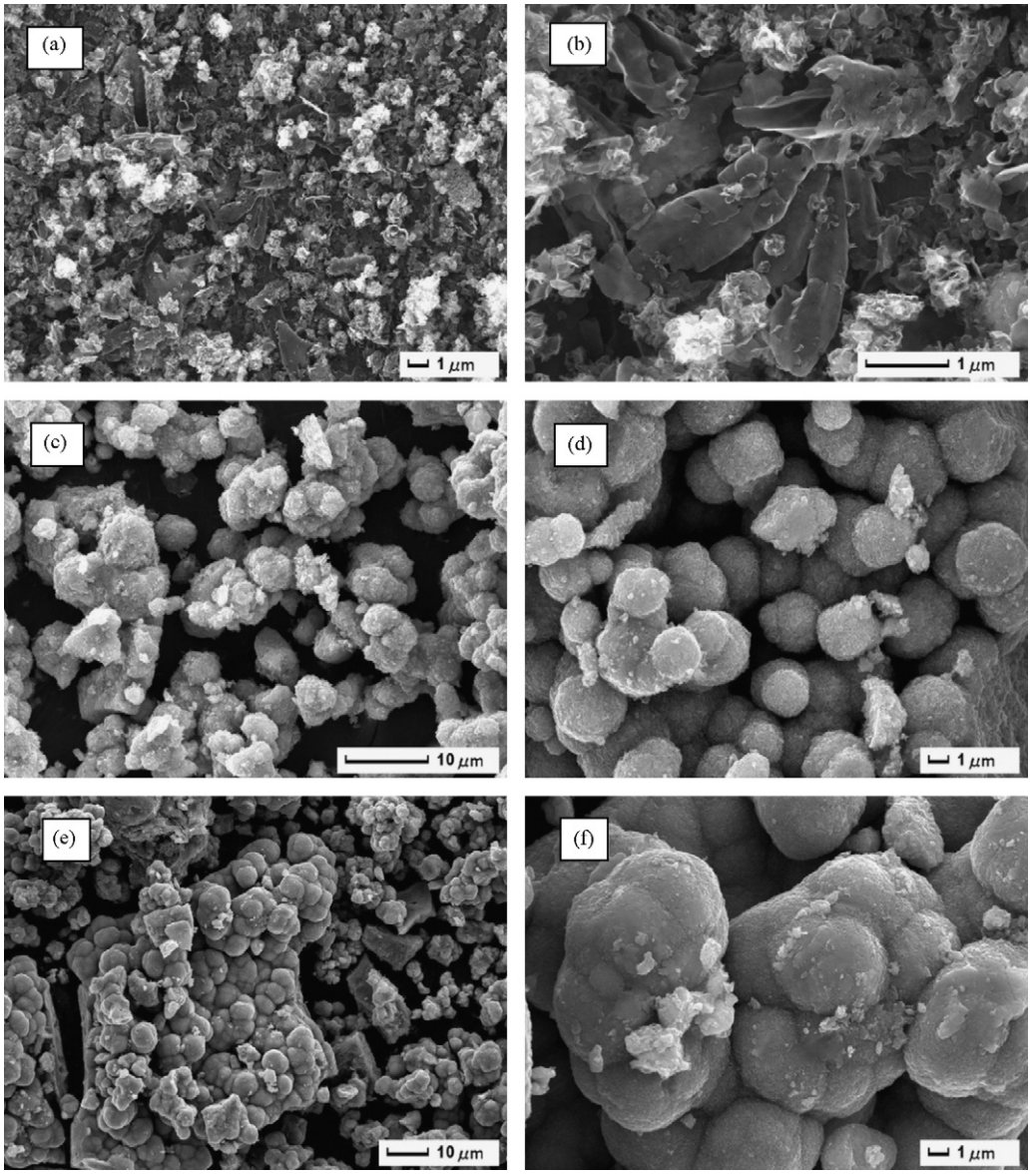

Fig. 6. SEM images of the obtained MoS_2 structures with different concentration of $C_{16}H_{36}BrN$: (a, b) 0, (c) 0.01, and (d) 0.15, and (e, f) 0.3 mol/L.

ment, the $(C_4H_9)_4NBr$ consisting of $(C_4H_9)_4N^+$ cation could form many vesicles in water at an appropriate concentration. On the other hand, the F^- ions can enhance the dissolution and reaction of MoO_3 by nucleophilic substitution [35], the reaction process can be expressed as follows:

$$2MoO_3 + 2F^- \rightarrow MoO_4{}^{2-} + MoO_2F_2 \quad (1)$$

$$MoO_2F_2 + 2H_2O \rightarrow MoO_4{}^{2-} + 2F^- + 4H^+ \quad (2)$$

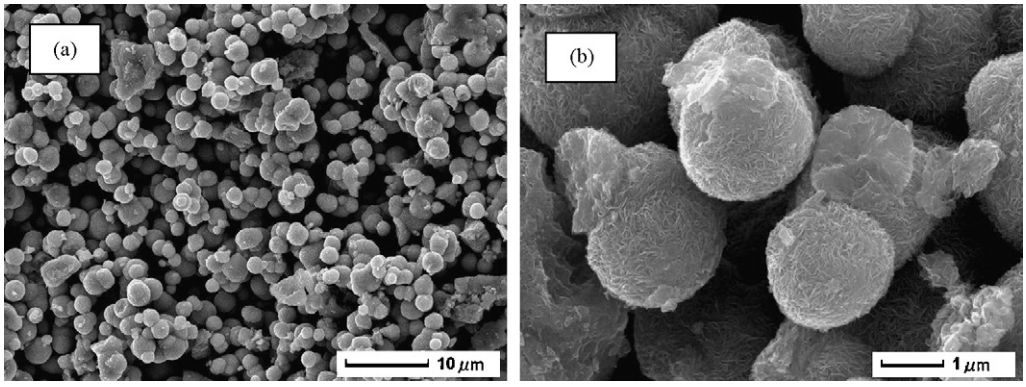

Fig. 7. SEM images of the obtained MoS_2 structures with pure ethanol as solvent. $C_{16}H_{36}BrN$: 0.03 mol/L.

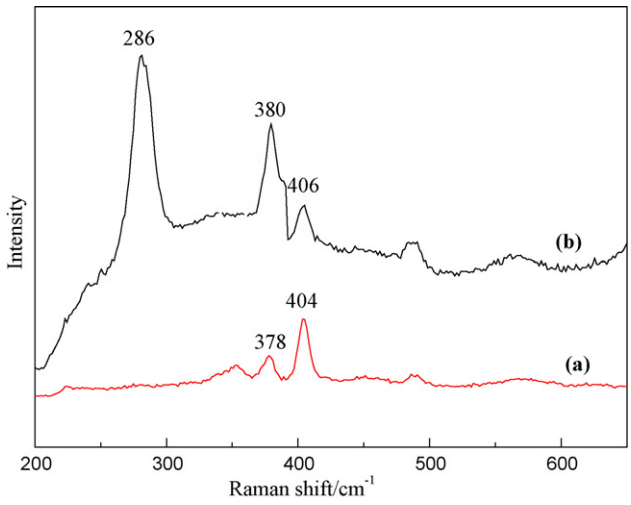

Fig. 8. Raman spectra of the as-prepared MoS_2 samples. (a) Before annealing treatment; (b) after annealing treatment.

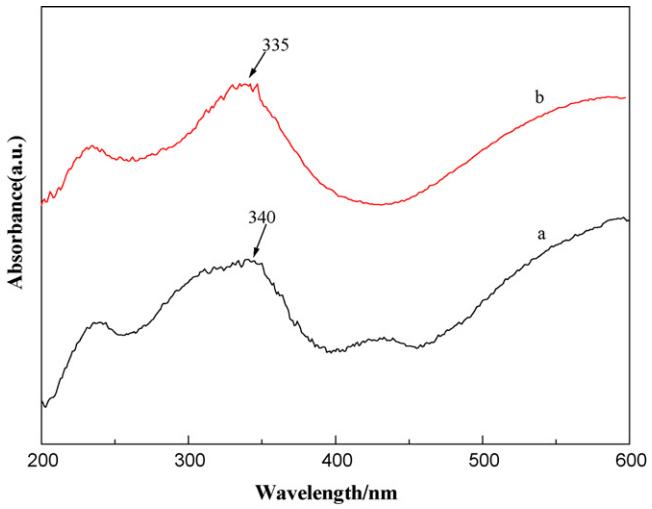

Fig. 9. UV–vis spectrum of the (a) bulk MoS_2; (b) as-prepared MoS_2 spheres.

It is well known that surfactant cation and metal oxo anion can co-organize to form periodic surfactant/inorganic composites materials, given that the charge density at the surfactant/inorganic interfaces matches well [36]. Thus the MoO_3 macrobelts (actually in the form of MoO_4^{2-} ions) of the precursor solution can absorb to the surface of these vesicles layer upon layer overlay by the electrostatic interaction. This process provides nucleation domains for the hydrothermal reaction between MoO_4^{2-} and S^{2-}, which were released from SCN^- upon a hydrolyzation process, serve as the reducing agent and sulfur source, the hollow spheres were formed during the hydrothermal reaction. Fig. 11a vividly displays the process of several MoO_3 macrobelts absorbed to the surface of two vesicles. From the above discussion, we can conclude that the possible reaction route may be expressed as follows:

$$NaSCN + 2H_2O + HCl \rightarrow NH_3\uparrow + H_2S\uparrow + CO_2\uparrow + NaCl \quad (3)$$

$$4MoO_3 + 9NaSCN + 10H_2O + 7HCl \rightarrow 4MoS_2 + NaSO_4 + 7NaCl + 9NH_3\uparrow + 9CO_2\uparrow \quad (4)$$

In order to further investigate the effect of the belt-like MoO_3 on the formation of the MoS_2 hollow microspheres, an experiment using commercial MoO_3 was carried out while other conditions were the same. Fig. 11b is a typical SEM image of the MoS_2 sample prepared by hydrothermal process with commercial MoO_3. It can be seen that there are no microspheres but

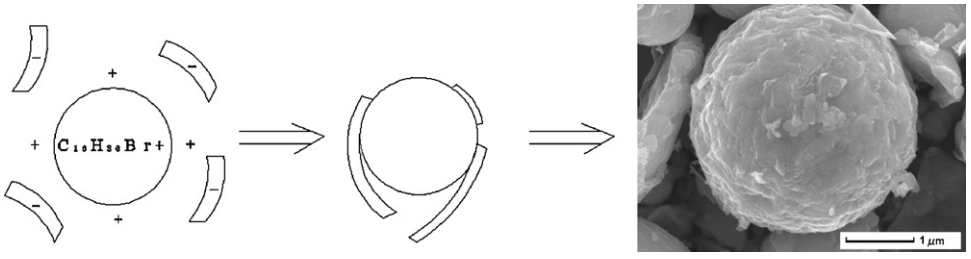

Fig. 10. Illustration of the formation mechanism of the microsphere MoS_2 structure.

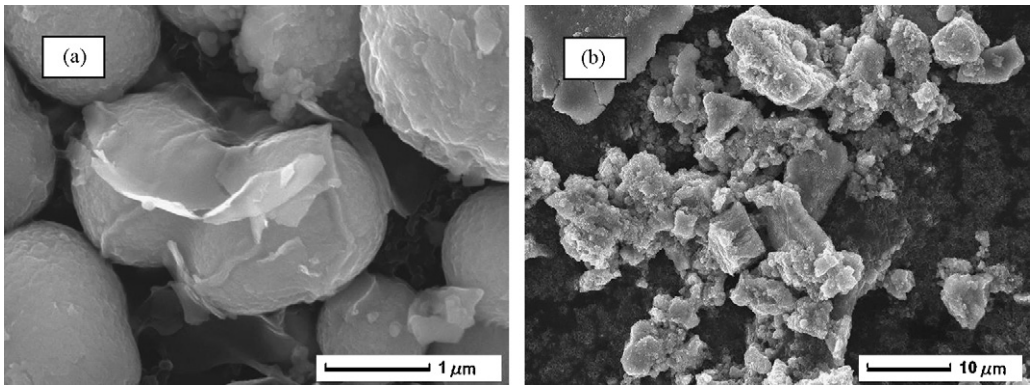

Fig. 11. (a) The process of the MoO_3 macrobelts absorbed to the surface of two vesicles. (b) SEM of the obtained MoS_2 structures with commercial MoO_3.

there are irregular particles. The above fact demonstrates that belt-like structure is key in the formation of the MoS_2 microspheres.

4. Conclusion

In conclusion, hollow MoS_2 microspheres with the diameters of 2–4 μm have been successfully synthesized via a facile hydrothermal route by adding tetrabutyl ammonium bromide as an additive. It was found that the as-prepared MoS_2 are hollowed and the shell is of a multi-layer structure. A possible growth mechanism for the hollow structure has also been tentatively proposed on the basis of the experimental results. On the one hand, the strategy described here is of particular interest for the synthesis of IF-MoS_2 spheres with hollow structure and might be extended to other layered materials.

Acknowledgments

The authors gratefully acknowledge the financial support from the National Nature Science Foundation of China (Grant No. 50471051).

References

[1] A. Kolmakov, Y.X. Zhang, G.S. Cheng, M. Moskovits, Adv. Mater. 15 (2003) 997–1000.
[2] X.F. Duan, Y. Huang, Y. Cui, J.F. Wang, C.M. Lieber, Nature 409 (2001) 66–69.
[3] F. Caruso, Chem. Eur. J. 6 (2000) 413–419.
[4] Z. Zhong, Y. Yin, B. Gates, Y. Xia, Adv. Mater. 12 (2000) 206–209.
[5] A.B. Bourlinos, M.A. Karakassides, D. Petridis, Chem. Commun. 16 (2001) 1518–1519.
[6] K.H. Rhodes, S.A. Davis, F. Caruso, B. Zhang, S. Mann, Chem. Mater. 12 (2000) 2832–2834.
[7] H.P. Cong, S.H. Yu, Adv. Funct. Mater. 17 (2007) 1814–1820.
[8] J.J. Zhu, S. Xu, H. Wang, J.M. Zhu, H.Y. Chen, Adv. Mater. 15 (2003) 156–159.
[9] C. Wang, K. Tang, Q. Yang, J. Hu, Y. Qian, J. Mater. Chem. 12 (2002) 2426–2429.
[10] R.K. Rana, Y. Mastai, A. Gedanken, Adv. Mater. 14 (2002) 1414–1418.
[11] S.W. Kim, M. Kim, W.Y. Lee, T. Hyeon, J. Am. Chem. Soc. 124 (2002) 7642–7643.
[12] Y.M. Li, W.Y. Li, S.L. Chou, J. Chen, J. Alloys Compd. 456 (2008) 339–343.
[13] H.T. Schmidt, A.E. Ostafin, Adv. Mater. 14 (2002) 532–535.
[14] J.X. Huang, Y. Xie, B. Li, Y. Liu, Y.T. Qian, S.Y. Zhang, Adv. Mater. 12 (2000) 808–812.
[15] M. Chhowalla, G. Amaratunga, Nature 407 (2000) 164–167.
[16] J. Chen, S.L. Li, Z.L.J. Tao, J. Alloys Compd. 356 (2003) 413–417.
[17] Q. Wang, J. Li, J. Phys. Chem. C 111 (2007) 1675–1682.
[18] V. Nemanic, M. Zumer, B. Zajec, J. Pahor, M. Remskar, A. Mrzel, P. Pajan, D. Mihalovic, Appl. Phys. Lett. 82 (2003) 4573–4575.
[19] M. Nath, A. Govindaraj, C.N.R. Rao, Adv. Mater. 13 (2001) 283–286.
[20] Y. Tian, Y. He, Y.F. Zhu, Chem. Lett. 32 (2003) 768–769.
[21] D. Duphil, S. Bastide, C. Levy-Clèment, J. Mater. Chem. 12 (2002) 2430–2432.
[22] M. Chhowalla, G.A.J. Amaratunga, Nature 407 (2000) 164–167.
[23] I. Uzcanga, I. Bezverkhyy, P. Afanasiev, C. Scott, M. Vrinat, Chem. Mater. 17 (2005) 3575–3577.
[24] C.M. Zelenski, P.K. Dorhout, J. Am. Chem. Soc. 120 (1998) 734–742.
[25] Q. Li, E.C. Walter, W.E. Van der Veer, B.J. Murray, J.T. Newberg, E.W. Bohannan, J.A. Switzer, J.C. Hemminger, R.M. Penner, J. Phys. Chem. B 109 (2005) 3169–3182.
[26] L.X. Chang, H.B. Yang, W.Y. Fu, J.Z. Zhang b, Q.J. Yu, H.Y. Zhu, J.J. Chen, R.H. Wei, Y.G. Sui, X.F. Pang, G.T. Zou, Mater. Res. Bull. 43 (2008) 2427–2433.
[27] J. Chen, S.L. Li, Q. Xu, K. Tanaka, Chem. Commun. 16 (2002) 1722–1723.
[28] Y. Feldman, E. Wasserman, D.J. Srolovitz, R. Tenne, Science 267 (1995) 222–225.
[29] T. Xia, Q. Li, X.D. Liu, J. Meng, X.Q. Cao, J. Phys. Chem. B 110 (2006) 2006–2012.
[30] X.L. Li, Y.D. Li, J. Phys. Chem. B 108 (2004) 13893–13900.
[31] A. Zak, Y. Feldman, V. Alperovich, V.R. Rosentsveig, R. Tenne, J. Am. Chem. Soc. 122 (2000) 11108–11116.
[32] A. Blanco, C. López, Adv. Mater. 18 (2006) 1593–1597.
[33] L. Verble, T.J. Wieting, Phys. Rev. B 12 (1971) 4286–4291.
[34] Nakashima, Kimizuka, J. Am. Chem. Soc. 125 (2003) 6386–6387.
[35] J.G. Yu, C.Y. Jimmy, W.K. Ho, L.W.X.C. Wang, J. Am. Chem. Soc. 126 (2004) 3422–3423.
[36] Q. Huo, D.I. Margolese, U. Ciesla, D.G. Demuth, Nature 368 (2004) 317–321.